Progress In Electromagnetics Research C, Vol. 109, 205–216, 2021

System of Material Objects in Electrodynamic Volumes

Mikhail V. Nesterenko*, Victor A. Katrich, Sergey L. Berdnik, and Victor I. Kijko

Abstract—In general, the problem of the excitation (radiation, scattering) of electromagnetic fields by a system of finite-dimensional material objects in arbitrary electrodynamic volumes is formulated. On the basis of the impedance concept, the problem is reduced to solving two-dimensional integral equations for electric surface currents on material objects. A physically correct transition from the obtained integral equations to a system of one-dimensional equations for currents on electrically thin impedance vibrators (monopoles) with electrophysical and geometric parameters that can be irregular along their length is made. As an example, a system of two monopoles with a variable surface impedance located in a rectangular waveguide is considered. The problem was solved by the generalized method of induced electromotive forces (EMF). A distinctive feature of this method is that the current distribution functions found by the asymptotic averaging method are used to solve integral equations for currents. The numerical and experimental results concerning electrodynamic characteristics of the structure under consideration are presented.

1. INTRODUCTION

At present, thin resonant vibrators and their systems allocated in rectangular waveguides are widely used as structural elements of resonant antenna-waveguide devices operating in microwave and extremely high frequency (EHF) ranges. Such devices may serve as structural components of coaxial-waveguide junctions, waveguide filters, matching and tuning elements, exciters for slot radiators, measuring probes, etc. [1–10].

The vibrators with distributed surface impedance can significantly improve electrodynamic characteristics of devices operating in infinite medium [11–18], in rectangular waveguides [18–21], and on spherical surface [22, 23]. A special place is occupied by vibrators with variable surface impedance located in free space [18, 24–27] or in electrodynamic volumes [18, 23, 28]. The vibrator with variable surface impedance can be used to control electrodynamic characteristics of radiators with fixed geometric dimensions [18, 23–28]. The results obtained in [24–28] are devoted to single vibrators excited in their center by a concentrated EMF in free space. The belt vibrators with real impedance specified by a step function of their length in rectangular waveguides are considered in [29]. The scattering problems of plane wave and TE_{10}-wave by single vibrator with variable impedance in free space and rectangular waveguides was considered in [18].

Recently, specialists have used commercial programs (Ansoft HFSS, FEKO, etc.) to calculate the electrodynamic characteristics of various waveguide structures [30]. However, these programs are not suitable in many cases, for example, for elements with variable distributed surface impedance along the vibrator length.

The present paper is aimed to solve a problem of the excitation of electromagnetic fields by a system of finite-dimensional material objects in arbitrary electrodynamic volumes and study electrodynamic characteristics of vibrator system with constant and variable distributed surface impedance in a rectangular waveguide.

Received 23 December 2020, Accepted 29 January 2021, Scheduled 7 February 2021

* Corresponding author: Mikhail V. Nesterenko (Mikhail.V.Nesterenko@gmail.com).

The authors are with the Department of Radiophysics, Biomedical Electronics and Computer Systems, V. N. Karazin Kharkiv National University, 4, Svobody Sq., Kharkiv 61022, Ukraine.

2. PROBLEM FORMULATION AND INITIAL INTEGRAL EQUATIONS

Let us formulate the problem of excitation (radiation, scattering) of electromagnetic fields in arbitrary electrodynamic volumes with material objects of finite dimensions. Consider a volume V, confined by a perfectly conducting surface S (or impedance or partially impedance surface S_Z) a part of which can be moved to infinity. The part of the surface S can be moved to infinity. The permittivity and permeability of medium in the volume V are $\varepsilon_1^v,\ \mu_1^v$. The volume V contains material objects enclosed in local volumes V_m $(m = 1, 2, \ldots, M)$ bounded by closed smooth surfaces S_m. The objects are characterized by homogeneous material parameters: permittivity ε_m, permeability μ_m, and conductivity σ_m (Fig. 1).

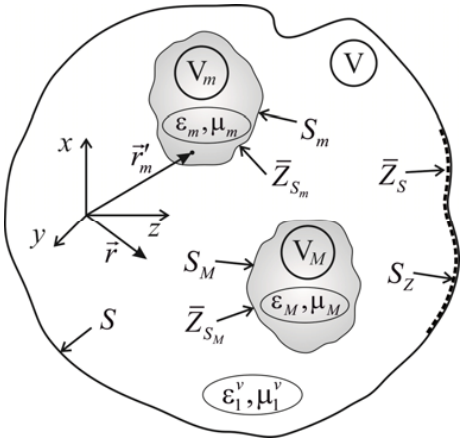

Figure 1. The problem geometry and corresponding notations.

The fields of external sources can be specified as the fields of electromagnetic waves incident on objects (scattering problem), as the fields of EMF applied to the objects, differing from zero only in some regions of volumes V_m (radiation problem), or as a combination of these fields. Let us assume that if monochromatic fields depend on time t as $e^{i\omega t}$ ($\omega = 2\pi f$ is the angular frequency and f is the frequency in Hz), the electromagnetic fields of specified extraneous sources in the volume V are $\{\vec{E}_0(\vec{r}),\ \vec{H}_0(\vec{r})\}$, where $\vec{r}$ is the radius vector of the observation point. The problem consists in finding the total electromagnetic fields $\{\vec{E}(\vec{r}),\ \vec{H}(\vec{r})\}$ in the volume V satisfying the Maxwell's equations and boundary conditions on the surfaces S_m and S.

The total electromagnetic field in the volume V can be easily expressed through tangential components of fields on the surface S_m. In the CGS-Gaussian system, the field can be represented as Kirchhoff-Kotler integral equations [18, 31]:

$$\begin{aligned}
\vec{E}(\vec{r}) \;=\; & \vec{E}_0(\vec{r}) + \frac{1}{4\pi i k \varepsilon_1^v}(\mathrm{graddiv} + k_1^2) \sum_{m=1}^{M} \int\limits_{S_m} \hat{G}^e(\vec{r}, \vec{r}_m')[\vec{n}_m, \vec{H}(\vec{r}_m')] d\vec{r}_m' \\
& - \frac{1}{4\pi} \mathrm{rot} \sum_{m=1}^{M} \int\limits_{S_m} \hat{G}^m(\vec{r}, \vec{r}_m')[\vec{n}_m, \vec{E}(\vec{r}_m')] d\vec{r}_m', \\
\vec{H}(\vec{r}) \;=\; & \vec{H}_0(\vec{r}) + \frac{1}{4\pi i k \mu_1^v}(\mathrm{graddiv} + k_1^2) \sum_{m=1}^{M} \int\limits_{S_m} \hat{G}^m(\vec{r}, \vec{r}_m')[\vec{n}_m, \vec{E}(\vec{r}_m')] d\vec{r}_m' \\
& + \frac{1}{4\pi} \mathrm{rot} \sum_{m=1}^{M} \int\limits_{S_m} \hat{G}^e(\vec{r}, \vec{r}_m')[\vec{n}_m, \vec{H}(\vec{r}_m')] d\vec{r}_m', \qquad (1)
\end{aligned}$$

where $k = 2\pi/\lambda$ is the wave number; λ is the wavelength in free space; $k_1 = k\sqrt{\varepsilon_1^v \mu_1^v}$ is the wave

number in the volume medium; $\vec{r}'_m$ are the radius vectors of source points located on surfaces S_m; $\vec{n}_m$ are unit vectors of external normals for these surfaces; and $\hat{G}^e(\vec{r},\vec{r}'_m)$, $\hat{G}^m(\vec{r},\vec{r}'_m)$ are electric and magnetic tensor Green's functions for vector Hertz potentials, satisfying the vector Helmholtz equation and corresponding boundary conditions on the surface S. The boundary conditions at infinite parts of surfaces transform into the Sommerfeld radiation condition.

The representation (1) can be applied to the solution of electrodynamic problem when some additional physical considerations are involved for determining the fields on object surfaces. For example, if currents induced on the well-conducting object ($\sigma_m \to \infty$) are concentrated on their surfaces, the Shchukin-Leontovich approximate impedance boundary conditions [18] can be used

$$[\vec{n}, \vec{E}(\vec{r})] = \bar{Z}_S(\vec{r})[\vec{n}, [\vec{n},\ \vec{H}(\vec{r})]], \tag{2}$$

where $\bar{Z}_S(\vec{r}) = \bar{R}_S(\vec{r}) + i\bar{X}_S(\vec{r}) = Z_S(\vec{r})/Z_0$ is the distributed surface impedance normalized to the characteristic impedance of free space $Z_0 = 120\pi$ Ohm. In general case, the impedance $\bar{Z}_S(\vec{r})$ may vary on the object surface. The boundary condition (2) is approximate in the sense that the solution of the electrodynamic problem with their use is the first term of the asymptotic expansion of the exact solution in powers of the small parameter $|\bar{Z}_S(\vec{r})| \ll 1$ [18]. In other words, the terms proportional to $|\bar{Z}_S(\vec{r})|^2$, $|\bar{Z}_S(\vec{r})|^3, \ldots$ are discarded from the solution.

The impedance boundary condition (2) allows us to change variable in the equation system (1) from the fields to surface currents. Without loss of generality, let us change variable for the case when two material objects located in the volume V. When the observation point is located on the surfaces S_1 or S_2, the following integral equation system relative to the density of the surface current $\vec{J}_{1,2}(\vec{r}_{1,2}) = (c/4\pi)[\vec{n}_{1,2},\ \vec{H}(\vec{r}_{1,2})]$ ($c \approx 2.998 \cdot 10^{10}$ cm/s is the speed of light in vacuum) on the surfaces S_1 and S_2 can be written as:

$$Z_{S1}(\vec{r}_1)\vec{J}_1(\vec{r}_1) = \vec{E}_0(\vec{r}) + \frac{1}{i\omega\varepsilon_1^v}(\mathrm{graddiv} + k_1^2)\left\{\int\limits_{S_1} \hat{G}^e(\vec{r},\vec{r}'_1)\vec{J}_1(\vec{r}'_1)d\vec{r}'_1 + \int\limits_{S_2} \hat{G}^e(\vec{r},\vec{r}'_2)\vec{J}_2(\vec{r}'_2)d\vec{r}'_2\right\}$$
$$+\frac{1}{4\pi}\mathrm{rot}\left\{\int\limits_{S_1} \hat{G}^m(\vec{r},\vec{r}'_1)Z_{S1}(\vec{r}'_1)[\vec{n}_1, \vec{J}_1(\vec{r}'_1)]d\vec{r}'_1 + \int\limits_{S_2} \hat{G}^m(\vec{r},\vec{r}'_2)Z_{S2}(\vec{r}'_2)[\vec{n}_2, \vec{J}_2(\vec{r}'_2)]d\vec{r}'_2\right\}, \tag{3a}$$

$$Z_{S2}(\vec{r}_2)\vec{J}_2(\vec{r}_2) = \vec{E}_0(\vec{r}) + \frac{1}{i\omega\varepsilon_1^v}(\mathrm{graddiv} + k_1^2)\left\{\int\limits_{S_2} \hat{G}^e(\vec{r},\vec{r}'_2)\vec{J}_2(\vec{r}'_2)d\vec{r}'_2 + \int\limits_{S_1} \hat{G}^e(\vec{r},\vec{r}'_1)\vec{J}_1(\vec{r}'_1)d\vec{r}'_1\right\}$$
$$+\frac{1}{4\pi}\mathrm{rot}\left\{\int\limits_{S_2} \hat{G}^m(\vec{r},\vec{r}'_2)Z_{S2}(\vec{r}'_2)[\vec{n}_2, \vec{J}_2(\vec{r}'_2)]d\vec{r}'_2 + \int\limits_{S_1} \hat{G}^m(\vec{r},\vec{r}'_1)Z_{S1}(\vec{r}'_1)[\vec{n}_1, \vec{J}_1(\vec{r}'_1)]d\vec{r}'_1\right\}, \tag{3b}$$

$$\vec{H}_0(\vec{r}) = -\frac{k}{\omega}\mathrm{rot}\left\{\int\limits_{S_1} \hat{G}^e(\vec{r},\vec{r}'_1)\vec{J}_1(\vec{r}'_1)d\vec{r}'_1 + \int\limits_{S_2} \hat{G}^e(\vec{r},\vec{r}'_2)\vec{J}_2(\vec{r}'_2)d\vec{r}'_2\right\}$$
$$+\frac{1}{i\omega\varepsilon_1^v}(\mathrm{graddiv} + k_1^2)\left\{\begin{array}{l}\displaystyle\int\limits_{S_1} \hat{G}^m(\vec{r},\vec{r}'_1)Z_{S1}(\vec{r}'_1)[\vec{n}_1,\ \vec{J}_1(\vec{r}'_1)]d\vec{r}'_1 \\ \displaystyle + \int\limits_{S_2} \hat{G}^m(\vec{r},\vec{r}'_2)Z_{S2}(\vec{r}'_2)[\vec{n}_2,\ \vec{J}_2(\vec{r}'_2)]d\vec{r}'_2\end{array}\right\}. \tag{3c}$$

3. INTEGRAL EQUATIONS FOR CURRENTS IN ELECTRICALLY THIN VIBRATORS

Direct solution of the equations system (3) for objects with complex surface shapes may encounter serious mathematical difficulties. However, the problem for impedance cylinders, whose cross-section

perimeter is small as compared to their length and the wavelength in the medium, the solution of the equation system can be greatly simplified. It is also possible to extend the boundary condition (2) for the cylindrical vibrator surfaces with an arbitrary distribution of the complex impedance for any structure of the exciting field and electrophysical characteristics of the vibrator material [18]. Formulas defining specific realizations of the surface vibrator impedance can be found in [18, 28].

Let us transform the equations system (3) for vibrators made of circular cylindrical wires with radii $r_{1,2}$ and lengths $2L_{1,2}$ satisfying the thin wire approximation

$$\frac{r_{1,2}}{2L_{1,2}} \ll 1, \quad \frac{r_{1,2}}{\lambda_1} \ll 1. \tag{4}$$

These inequalities make it possible to assume that the electric currents induced in the vibrators can be represented as

$$\vec{J}_{1(2)}(\vec{r}_{1(2)}) = \vec{e}_{s_{1(2)}} J_{1(2)}(s_{1(2)}) \psi_{1(2)}(\rho_{1(2)}, \varphi_{1(2)}), \tag{5}$$

where $\vec{e}_{s_{1(2)}}$ are unit vectors directed along the vibrator axes; $s_{1(2)}$ are local coordinates associated with the vibrators axes; $\psi_{1(2)}(\rho_{1(2)}, \varphi_{1(2)})$ are functions of transverse polar coordinates $\rho_{1(2)}, \varphi_{1(2)}$. The functions $\psi_{1(2)}(\rho_{1(2)}, \varphi_{1(2)})$ satisfy normalization conditions $\int\limits_{\perp_{1(2)}} \psi_{1(2)}(\rho_{1(2)}, \varphi_{1(2)}) \rho_{1(2)} d\rho_{1(2)} d\varphi_{1(2)} = 1$ and boundary conditions for the vibrator currents

$$J_{1(2)}(\pm L_{1(2)}) = 0\,. \tag{6}$$

Let us project Equations (3a) and (3b) on the vibrator axes taking into account the relations in Eqs. (5)–(6) and the inequality $[\vec{n}_{1(2)}, \vec{J}_{1(2)}(\vec{r}_{1(2)})] \ll 1$, which follows from relations (4). Then, the integral equation system for the vibrator currents with account of interaction between the vibrators can be written as:

$$\left(\frac{d^2}{ds_1^2} + k_1^2\right) \left\{ \begin{array}{l} \int\limits_{-L_1}^{L_1} J_1(s_1') G_{s_1}(s_1, s_1') ds_1' \\ + \int\limits_{-L_2}^{L_2} J_2(s_2') G_{s_2}(s_1, s_2') ds_2' \end{array} \right\} = -i\omega\varepsilon_1^v \left[E_{0s_1}(s_1) - z_{i1}(s_1) J_1(s_1)\right], \tag{7a}$$

$$\left(\frac{d^2}{ds_2^2} + k_1^2\right) \left\{ \begin{array}{l} \int\limits_{-L_2}^{L_2} J_2(s_2') G_{s_2}(s_2, s_2') ds_2' \\ + \int\limits_{-L_1}^{L_1} J_1(s_1') G_{s_1}(s_2, s_1') ds_1' \end{array} \right\} = -i\omega\varepsilon_1^v \left[E_{0s_2}(s_2) - z_{i2}(s_2) J_2(s_2)\right], \tag{7b}$$

where $z_{i1(2)}(s_{1(2)})$ are internal linear impedances ([Ohm/m]) of vibrators $Z_{S1(2)}(\vec{r}_{1(2)}) = 2\pi r_{1(2)} z_{i1(2)}(\vec{r}_{1(2)})$, $E_{0s_{1(2)}}(s_{1(2)})$ are projections of extraneous sources fields on the vibrator axes; $s_1 = -L_1$ and $s_2 = -L_2$ are coordinates of mirror images of the vibrator ends in the lower wide wall of the waveguide; and $G_{s_{1,2}}(s_{1,2}, s_{1,2}')$ are the tensors Green's functions components of the volume V. Since the form of the Green functions was not specified in Equation (7), they are valid for any electrodynamic volume V if the Green's functions are known or can be constructed for this volume.

4. TWO IMPEDANCE VIBRATORS IN RECTANGULAR WAVEGUIDE

Consider a hollow ($\varepsilon_1^v = \mu_1^v = 1$) infinite rectangular waveguide with perfectly conducting walls where two thin asymmetric vibrators (monopoles) with variable surface impedance are located (Fig. 2). The waveguide cross-section is $\{a \times b\}$, and the vibrator radii and lengths are $r_{1,2}$ and $L_{1,2}$. The TE_{10}-wave propagates in the waveguide from the direction $z = -\infty$.

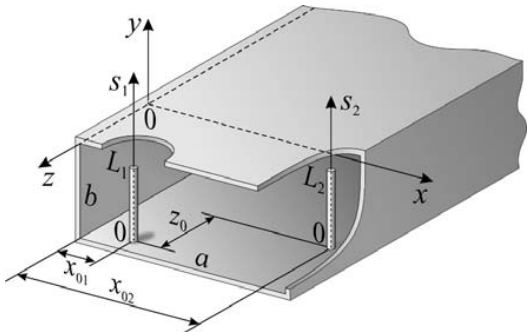

Figure 2. The two vibrators system in the rectangular waveguide.

The solution of equations system in Eq. (7) will be sought by the generalized method of induced EMF [18], using functions $J_{1(2)}(s_{1(2)}) = J^0_{1(2)} f_{1(2)}(s_{1(2)})$ as approximating expressions for vibrator currents. In these expressions, $J^0_{1(2)}$ are unknown current amplitudes, and $f_{1(2)}(s_{1(2)})$ are predefined current distribution functions, which can be obtained by solving the equation for the current on stand-alone vibrators by averaging method [4, 18, 20, 21]. When the structure is excited by the TE_{10}-wave, the distribution function can be presented as:

$$f_1(s_1) = \cos\tilde{k}_1 s_1 - \cos\tilde{k}_1 L_1, \tag{8a}$$

$$f_2(s_2) = \cos\tilde{k}_2 s_2 - \cos\tilde{k}_2 L_2, \tag{8b}$$

where $\tilde{k}_{1(2)} = k - \frac{i2\pi z^{av}_{i1(2)}}{Z_0\Omega_{1(2)}}$, $z^{av}_{i1(2)} = \frac{1}{2L_{1(2)}} \int\limits_{-L_{1(2)}}^{L_{1(2)}} z_{i1(2)}(s_{1(2)})ds_{1(2)}$ are internal impedances averaged over the vibrator lengths and $\Omega_{1(2)} = 2\ln(2L_{1(2)}/r_{1(2)})$.

First, let us multiply Equations (7a) and (7b) by functions $f_1(s_1)$ and $f_2(s_2)$, respectively, and then integrate the results over the vibrator lengths. Thus, a system of linear algebraic equations (SLAE) are derived whose solution defines the current amplitudes $J^0_{1,2}$:

$$\begin{aligned} J^0_1\left(Z_{11} + F^{\bar{Z}}_1\right) + J^0_2 Z_{12} &= -\frac{i\omega}{2k}E_1, \\ J^0_2\left(Z_{22} + F^{\bar{Z}}_2\right) + J^0_1 Z_{21} &= -\frac{i\omega}{2k}E_2, \end{aligned} \tag{9}$$

where

$$\begin{aligned} Z_{11(22)} &= \frac{4\pi}{ab}\sum_{m=1}^{\infty}\sum_{n=0}^{\infty}\frac{\varepsilon_n\left(k^2-k_y^2\right)\tilde{k}^2_{1(2)}}{kk_z\left(\tilde{k}^2_{1(2)}-k_y^2\right)^2}e^{-k_z r_{1(2)}}\sin^2 k_x x_{01(02)} \\ &\quad\times\left[\sin\tilde{k}_{1(2)}L_{1(2)}\cos k_y L_{1(2)} - \left(\tilde{k}_{1(2)}/k_y\right)\cos\tilde{k}_{1(2)}L_{1(2)}\sin k_y L_{1(2)}\right]^2, \\ Z_{12(21)} &= \frac{4\pi}{ab}\sum_{m=1}^{\infty}\sum_{n=0}^{\infty}\frac{\varepsilon_n\left(k^2-k_y^2\right)\tilde{k}_1\tilde{k}_2 e^{-k_z r_{2(1)}}}{kk_z\left(\tilde{k}_1^2-k_y^2\right)\left(\tilde{k}_2^2-k_y^2\right)}\sin k_x x_{01}\sin k_x x_{02} \\ &\quad\times\left[\sin\tilde{k}_1 L_1\cos k_y L_1 - \left(\tilde{k}_1/k_y\right)\cos\tilde{k}_1 L_1\sin k_y L_1\right] \\ &\quad\times\left[\sin\tilde{k}_2 L_2\cos k_y L_2 - \left(\tilde{k}_2/k_y\right)\cos\tilde{k}_2 L_2\sin k_y L_2\right], \\ E_{1(2)} &= 2H_0\frac{k}{k_g\tilde{k}_{1(2)}}\sin\frac{\pi}{a}x_{01(02)} f\left(\tilde{k}_{1(2)}L_{1(2)}\right), \\ f\left(\tilde{k}_{1(2)}L_{1(2)}\right) &= \sin\tilde{k}_{1(2)}L_{1(2)} - \tilde{k}_{1(2)}L_{1(2)}\cos\tilde{k}_{1(2)}L_{1(2)}, \end{aligned} \tag{10}$$

$$F_{1(2)}^{\bar{Z}} = -\frac{i}{r_{1(2)}} \int_0^{L_{1(2)}} f_{1(2)}^2(s_{1(2)}) \bar{Z}_{S1(2)}(s_{1(2)}) ds_{1(2)}. \tag{11}$$

The following notation in Equations (10) and (11) are accepted: $\varepsilon_n = \begin{cases} 1, & n=0 \\ 2, & n \neq 0 \end{cases}$, $k_x = \frac{m\pi}{a}$ $k_y = \frac{n\pi}{b}$, m and n are integers; $k_z = \sqrt{k_x^2 + k_y^2 - k^2}$, $k_g = 2\pi/\lambda_g = \sqrt{k^2 - (\pi/a)^2}$; λ_g is the wavelength in the waveguide; $\bar{Z}_{S1(2)}(s_{1(2)}) = \bar{R}_{S1(2)} + i\bar{X}_{S1(2)}\phi(s_{1(2)})$ are the complex distributed surface impedances; $\phi(s_{1(2)})$ are the predefined functions; and H_0 is the amplitude of the incident TE_{10}-wave.

The analytical solution of the equation system in Eq. (9) has the following form:

$$\begin{aligned} J_1^0 &= -\frac{i\omega}{2k} \frac{E_1(Z_{22}+F_2^z) - E_2 Z_{12}}{(Z_{11}+F_1^z)(Z_{22}+F_2^z) - Z_{21}Z_{12}} = -\frac{i\omega}{2k}\tilde{J}_1^0, \\ J_2^0 &= -\frac{i\omega}{2k} \frac{E_2(Z_{11}+F_1^z) - E_1 Z_{21}}{(Z_{11}+F_1^z)(Z_{22}+F_2^z) - Z_{21}Z_{12}} = -\frac{i\omega}{2k}\tilde{J}_2^0. \end{aligned} \tag{12}$$

The final expressions for the vibrator currents can be written using Equations (8) and (12) as

$$J_{1(2)}(s_{1(2)}) = -\frac{i\omega}{2k}\tilde{J}_{1(2)}^0 \left(\cos\tilde{k}_{1(2)}s_{1(2)} - \cos\tilde{k}_{1(2)}L_{1(2)}\right). \tag{13}$$

The energy characteristics of the structure: the reflection S_{11} and S_{12} transmission coefficients can be determined as:

$$S_{11} = -\frac{4\pi i}{abkk_g}\left\{\frac{k^2}{\tilde{k}_1}\tilde{J}_1^0 \sin\left(\frac{\pi x_{01}}{a}\right) f\left(\tilde{k}_1 L_1\right) e^{-ik_g z_0} + \frac{k^2}{\tilde{k}_2}\tilde{J}_2^0 \sin\left(\frac{\pi x_{02}}{a}\right) f(\tilde{k}_2 L_2)\right\} e^{2ik_g z}, \tag{14}$$

$$S_{12} = 1 + \frac{4\pi i}{abkk_g}\left\{\frac{k^2}{\tilde{k}_1}\tilde{J}_1^0 \sin\left(\frac{\pi x_{01}}{a}\right) f\left(\tilde{k}_1 L_1\right) e^{ik_g z_0} + \frac{k^2}{\tilde{k}_2}\tilde{J}_2^0 \sin\left(\frac{\pi x_{02}}{a}\right) f(\tilde{k}_2 L_2)\right\}. \tag{15}$$

The voltage standing wave ratio is defined by the formula VSWR $= (1+|S_{11}|)/(1-|S_{11}|)$.

5. NUMERICAL AND EXPERIMENTAL RESULTS

Consider several impedance distributions defined by linear functions of coordinates $s_{1(2)}$: constant $\phi_0(s_{1(2)}) = 1$, decreasing $\phi_1(s_{1(2)}) = 2[1 - (s_{1(2)}/L_{1(2)})]$ and increasing $\phi_2(s_{1(2)}) = 2(s_{1(2)}/L_{1(2)})$ functions with equal averages along the vibrator length, $\overline{\phi_{0,1,2}(s_{1(2)})} = 1$. Substituting the distribution functions, $\phi_0(s_{1(2)})$, $\phi_1(s_{1(2)})$, and $\phi_2(s_{1(2)})$ into the expression (11), the functions $F_{1(2)}^{\bar{Z}0}$, $F_{1(2)}^{\bar{Z}1}$, and $F_{1(2)}^{\bar{Z}2}$ can be obtained in the form:

$$\begin{aligned} F_{1(2)}^{\bar{Z}0} &= -\frac{2i\left(\bar{R}_{S1(2)} + i\bar{X}_{S1(2)}\right)}{\tilde{k}_{1(2)}^2 L_{1(2)} r_{1(2)}} \left[\begin{array}{l} \left(\frac{\tilde{k}_{1(2)}L_{1(2)}}{2}\right)^2 \left(2 + \cos 2\tilde{k}_{1(2)}L_{1(2)}\right) \\ -(3/8)\tilde{k}_{1(2)}L_{1(2)} \sin 2\tilde{k}_{1(2)}L_{1(2)} \end{array}\right] \\ &= \tilde{F}_{1(2)}^{\bar{Z}}\left(\bar{R}_{S1(2)} + i\bar{X}_{S1(2)}\right)\Phi_{1(2)}, \end{aligned} \tag{16}$$

$$F_{1(2)}^{\bar{Z}1} = \tilde{F}_{1(2)}^{\bar{Z}} \left\{ \bar{R}_{S1(2)}\Phi_{1(2)} + i\bar{X}_{S1(2)} \left[\begin{array}{l} \left(\frac{\tilde{k}_{1(2)}L_{1(2)}}{2}\right)^2 \left(2 + \cos 2\tilde{k}_{1(2)}L_{1(2)}\right) \\ -(7/4)\sin^2\tilde{k}_{1(2)}L_{1(2)} - 2\left(\cos\tilde{k}_{1(2)}L_{1(2)} - 1\right) \end{array}\right] \right\}, \tag{17}$$

and

$$F_{1(2)}^{\bar{Z}2} = \tilde{F}_{1(2)}^{\bar{Z}} \left\{ \bar{R}_{S1(2)}\Phi_{1(2)} + i\bar{X}_{S1(2)} \left[\begin{array}{l} \left(\frac{\tilde{k}_{1(2)}L_{1(2)}}{2}\right)^2 \left(2 + \cos 2\tilde{k}_{1(2)}L_{1(2)}\right) + (7/4)\sin^2\tilde{k}_{1(2)}L_{1(2)} \\ -(3/4)\tilde{k}_{1(2)}L_{1(2)} \sin 2\tilde{k}_{1(2)}L_{1(2)} + 2\left(\cos\tilde{k}_{1(2)}L_{1(2)} - 1\right) \end{array}\right] \right\}. \tag{18}$$

As from Eqs. (16)–(18), the functions $F_{1(2)}^{\bar{Z}0,1,2}$ obtained for different impedance distributions differ from each other, despite the equal averages of functions $\phi_{0,1,2}(s_{1(2)})$. Therefore, it can be concluded that although the functions $f_{1(2)}(s_{1(2)}) = \cos\tilde{k}_{1(2)}s_{1(2)} - \cos\tilde{k}_{1(2)}L_{1(2)}$ in the formulas for the current coincide for all three impedance distributions, the current amplitudes and hence, the energy characteristics of the vibrator-waveguide system are significantly different for all three impedance distribution functions.

The simulation results presented in Figs. 3–8 were obtained for the radiator system with following parameters: $a = 58.0\,\text{mm}$, $b = 25.0\,\text{mm}$, $L_{1,2} = 15.0\,\text{mm}$, $r_{1,2}/2L_{1,2} = 0.07$, and $r_{1,2}/\lambda$ is in the range from 0.02 to 0.03. Such a vibrator length was selected to reduce the probability of electrical breakdown in the waveguide operating at high radiated power. The resonant vibrator wavelengths for various values of the impedance $\bar{X}_S$ are represented in Table 1.

Table 1. The resonant vibrator wavelengths.

$\bar{X}_S$	λ_{res}, mm	$\lvert\bar{X}_S\rvert^2\rvert_{\lambda=\lambda_{res}}$	$\lambda_G^{res} = \frac{2\pi}{\sqrt{k_{res}^2-(\pi/a)^2}}$, mm $(k_{res} = 2\pi/\lambda_{res})$	$\frac{\lambda_G^{res}}{4}$, mm	$\frac{\lambda_G^{res}}{2}$, mm	$\frac{3\lambda_G^{res}}{4}$, mm
$\frac{-0.03}{kr}$	66	0.025	80	20	40	60
0	72	0	92	23	46	69
$kr\ln(4.0)\phi_2(s)$	80	0.047	108	27	54	81
$kr\ln(4.0)$ $kr\ln(2.7)\phi_1(s)$	84	0.043 0.022	120	30	60	90
$kr\ln(4.0)\phi_1(s)$	88	0.039	136	34	68	102
$kr\ln(8.0)\phi_1(s)$	96	0.074	170	42.5	85	127.5

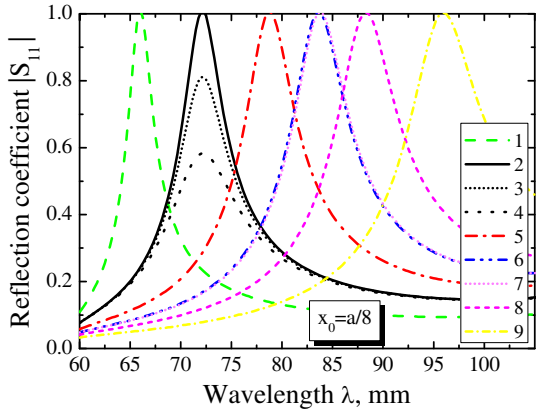

Figure 3. The reflection coefficient $|S_{11}|$ as a function of wavelength for the waveguide structure with single monopoles: 1 — $\bar{X}_S = -0.03/(kr)$, 2 — $\bar{Z}_S = 0$, 3 — $\bar{Z}_S = 0.01$, 4 — $\bar{Z}_S = 0.03$, 5 — $\bar{X}_S = kr\ln(4.0)\phi_2(s)$, 6 — $\bar{X}_S = kr\ln(4.0)$, 7 — $\bar{X}_S = kr\ln(2.7)\phi_1(s)$, 8 — $\bar{X}_S = kr\ln(4.0)\phi_1(s)$, 9 — $\bar{X}_S = kr\ln(8.0)\phi_1(s)$.

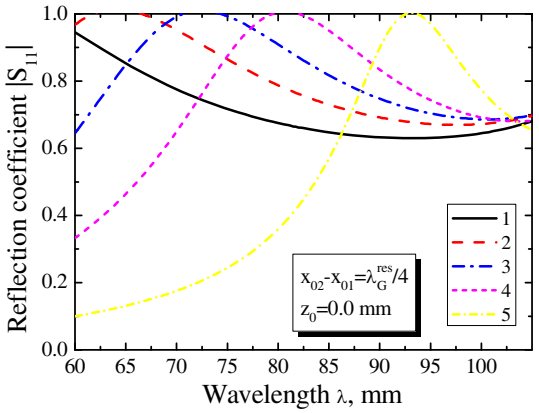

Figure 4. The reflection coefficient $|S_{11}|$ as a function of wavelength for the waveguide structure with two monopoles: 1 — $\bar{X}_{S1,2} = 0$, 2 — $\bar{X}_{S1,2} = kr_{1,2}\ln(4.0)\phi_2(s_{1,2})$, 3 — $\bar{X}_{S1,2} = kr_{1,2}\ln(4.0)$, 4 — $\bar{X}_{S1,2} = kr_{1,2}\ln(4.0)\phi_1(s_{1,2})$, 5 — $\bar{X}_{S1,2} = kr_{1,2}\ln(8.0)\phi_1(s_{1,2})$.

The curves of the reflection coefficient modulus $|S_{11}| = f(\lambda)$ in the waveguide for single monopoles are plotted in Fig. 3 for the various value, type, and distribution functions of the surface impedance. The impedance of various types can be realized as follows: an active impedance $\bar{R}_S > 0$ by a dielectric

cylinder with a metal coating thinner than skin layer; an inductive impedance $\bar{X}_S > 0$ by a metal cylinder with magnetodielectric coating or corrugated metal cylinder; and a capacitive impedance $\bar{X}_S < 0$ by a layered metal-dielectric cylinder. As can be seen from Fig. 3, the vibrators can be resonantly tuned ($|S_{11}|_{\max}$, $\arg S_{11} = 0$) at any frequency from the single mode range of waveguide operation. As expected, the resonant wavelength λ_{res} for vibrator with equal length can be decreased or increased if the capacitive or inductive impedance is applied. At the same time, the active impedance $\bar{R}_S$ decreases the reflection coefficient $|S_{11}|_{\max}$, but it practically does not affect the vibrator resonant wavelength λ_{res} (curves 3.4). All simulation results were obtained with $\bar{R}_S = 0.0001$. The relative stopband $\Delta\lambda/\lambda_{res}$ at the half power level ($0.707|S_{11}|_{\max}$) is in the range from 4% to 8%.

When the second monopole is placed in the plane of the waveguide cross-section symmetrically relative to its longitudinal axis at a distance $\lambda_G^{res}/4$ from the first vibrator, the ratio $\Delta\lambda/\lambda_{res}$ significantly increases up to 15% or 50% in the long-wave or short-wave parts of the waveguide operating range. At the same time, the common resonant wavelength of the vibrator system simultaneously reduces (Fig. 4).

When the monopoles are allocated from one another in the plane $\{x0y\}$ at distances other than $\lambda_G^{res}/4$, the second reflection and transmission resonances are observed (Fig. 5). In this case, the width of the reflection resonance curves for the symmetric vibrator allocation ($x_{01} = a - x_{02}$) shown in Fig. 5(a) is greater than that for asymmetric allocation ($x_{01} \neq a - x_{02}$) shown in Fig. 5(b). The same curve shapes are also observed for the transmission resonance if impedance distributions are increasing functions, while for the constant and increasing impedance distributions, the curves become wider for the asymmetric arrangement of vibrators.

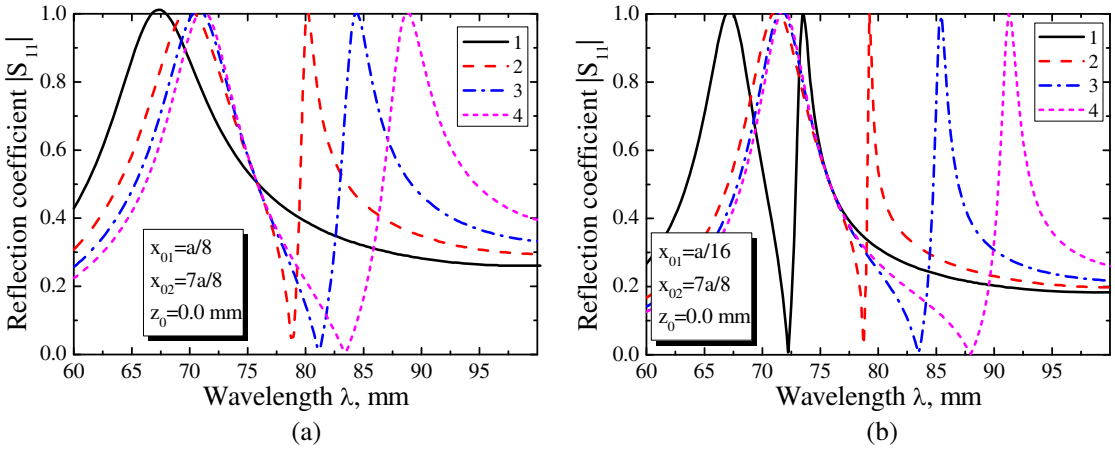

Figure 5. The reflection coefficient $|S_{11}|$ as a function of wavelength for the waveguide structure with two monopoles: 1 — $\bar{X}_{S1} = 0$, $\bar{X}_{S2} = 0$; 2 — $\bar{X}_{S1} = kr_1 \ln(4.0)\phi_2(s_1)$, $\bar{X}_{S2} = 0$; 3 — $\bar{X}_{S1} = kr_1 \ln(4.0)$, $\bar{X}_{S2} = 0$; 4 — $\bar{X}_{S1} = kr_1 \ln(4.0)\phi_1(s_1)$, $\bar{X}_{S2} = 0$.

Various combinations of impedance magnitude, type, and distributions cause significant changes reflection and transmission resonance positions in the operating wavelength range (Fig. 6). With equal impedances the monopoles resonate at the same wavelength, therefore only one reflection resonance is observed (curve 3).

If the resonant vibrator wavelengths are positioned at different ends of the waveguide operating range, the reflection resonances are also observed at these wavelengths. The resonant curves of the transmission coefficient in the long-wave part of the operating wavelength for the asymmetric monopole arrangement are much narrower as compared with that for the symmetric monopole arrangement (Fig. 7). Such shape of curves can be explained by the different wavelength dependence for the vibrators with inductive and capacitive impedances.

When one of the vibrators is displaced relative to another along the waveguide longitudinal axis at $n\lambda_G^{res}/4$ ($n = 1, 3, 5, \ldots$), the steepness of resonance curves significantly increases as compared to that for the single monopole and system of two monopoles located in the plane $\{x0y\}$. The steepness increases in greater degree for larger n (Fig. 8). In this case, two transmission resonances are observed

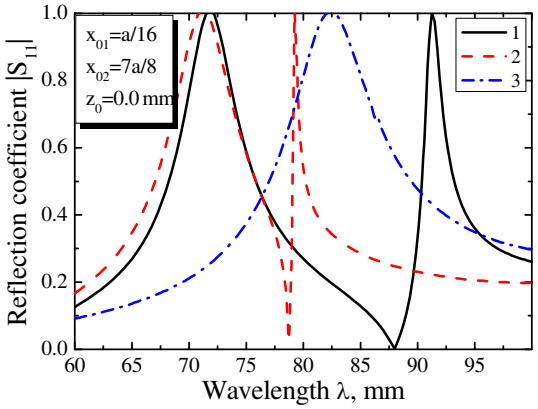

Figure 6. The reflection coefficient $|S_{11}|$ as a function of wavelength for the waveguide structure with two monopoles: 1 — $\bar{X}_{S1} = kr_1 \ln(4.0)\phi_1(s_1)$, $\bar{X}_{S2} = 0$; 2 — $\bar{X}_{S1} = kr_1 \ln(4.0)\phi_2(s_1)$, $\bar{X}_{S2} = 0$; 3 — $\bar{X}_{S1} = kr_1 \ln(4.0)$, $\bar{X}_{S2} = kr_2 \ln(2.7)\phi_1(s_2)$.

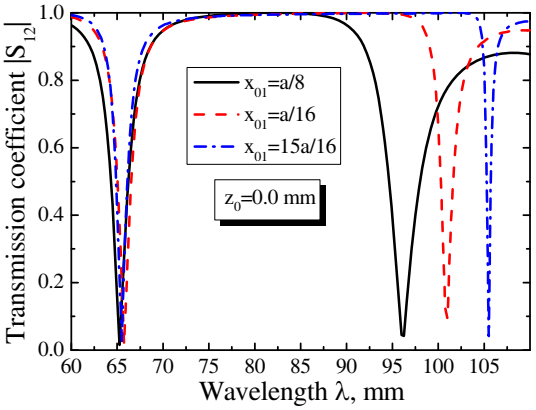

Figure 7. The transmission coefficient $|S_{12}|$ for the system with two monopoles as the function of wavelength ($x_{02} = 7a/8$): $\bar{X}_{S1} = kr_1 \ln(8.0)\phi_1(s_1)$, $\bar{X}_{S2} = -0.03/(kr_2)$.

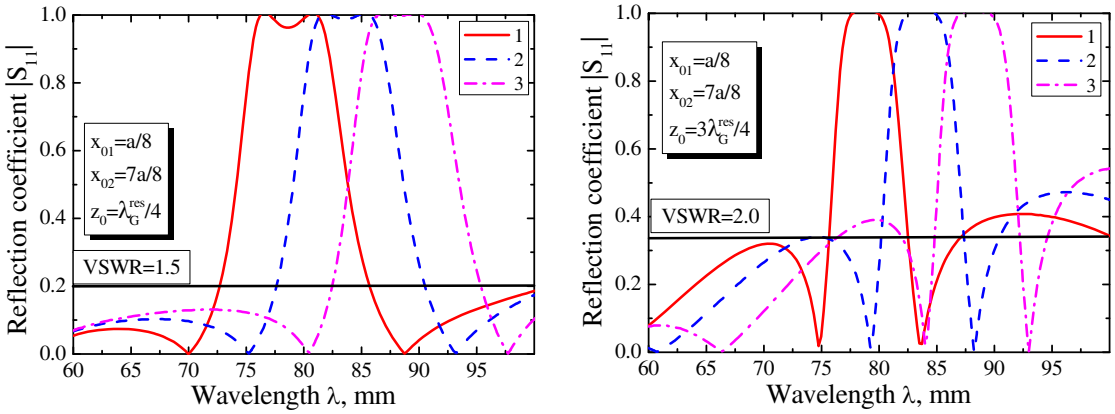

Figure 8. The reflection coefficient $|S_{11}|$ as a function of wavelength for the waveguide structure with two monopoles: 1 — $\bar{X}_{S1,2} = kr_{1,2} \ln(4.0)\phi_2(s_{1,2})$, 2 — $\bar{X}_{S1,2} = kr_{1,2} \ln(4.0)$, 3 — $\bar{X}_{S1,2} = kr_{1,2} \ln(4.0)\phi_1(s_{1,2})$.

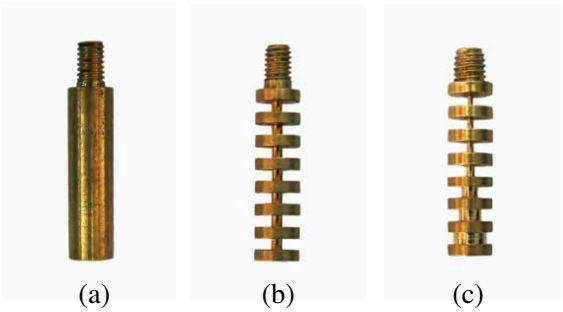

Figure 9. Experimental monopole samples: (a) solid brass cylinder with $r = 2.0$ mm; (b) corrugated brass cylinder with outer and inner radii $r = 2.0$ mm, $r_i = 0.5$ mm and cell length equal to 2.0 MM; (c) a corrugated brass cylinder with outer radius equal to 2.0 mm and variable inner radius $r_i(s) = r \exp[-\ln(r/r_i)\phi_1(s)]$.

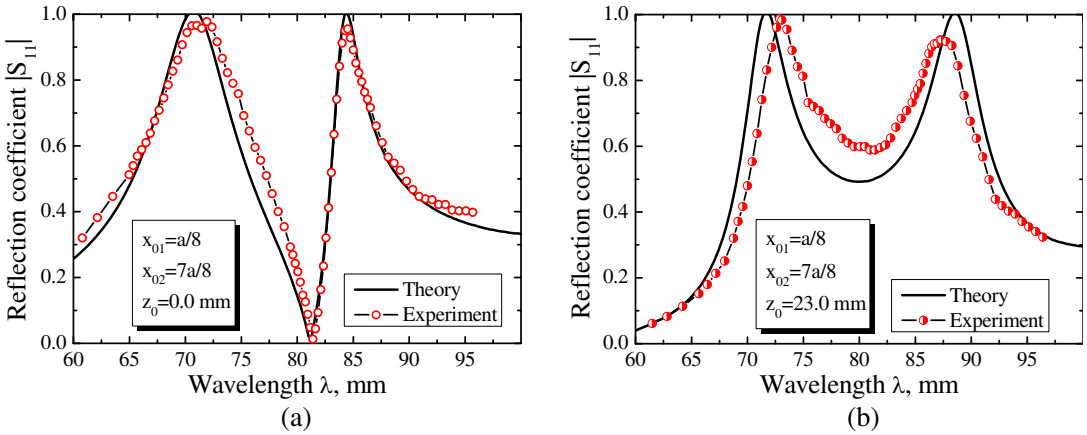

Figure 10. Theoretical and experimental reflection coefficients $|S_{11}|$ as functions of wavelength for the system with two monopoles: (a) $\bar{X}_{S1} = kr_1 \ln(4.0)$, $\bar{X}_{S2} = 0$; (b) $\bar{X}_{S1} = kr_1 \ln(4.0)\phi_1(s_1)$, $\bar{X}_{S2} = 0$.

on both sides of the reflection resonances.

Experimental measurements of reflection coefficient $|S_{11}|$ were carried out by using monopole samples shown in Fig. 9. As can be seen from Fig. 10, the calculated and experimental results are in satisfactory agreement.

6. CONCLUSION

It has been shown that distributed surface impedance of single vibrator with fixed geometric dimensions allocated in the rectangular waveguide can be tuned into resonance at any wavelength from the operating waveguide range. Various combinations of impedance magnitude, type, and distribution functions cause significant changes in positions of reflection and transmission resonances in the operating wavelength range. The surface impedance of the inductive type, especially with the increasing distribution function makes it possible to use vibrators and multi-element vibrator systems as resonant elements in low-profile waveguides. Comparison of the calculated results with experimental data for the two impedance monopoles system in the rectangular waveguide confirms the adequacy of the proposed mathematical model to real physical processes. The obtained results can be used to developing and designing various antenna-waveguide devices with resonant vibrators.

REFERENCES

1. Al-Hakkak, M. J., "Experimental investigation of the input-impedance characteristics of an antenna in a rectangular waveguide," *Electronics Letters*, Vol. 5, 513–514, 1969.
2. Craven, G. F. and C. K. Mok, "The design of evanescent mode waveguide bandpass filters for a prescribed insertion loss characteristic," *IEEE Trans. Microwave Theory Tech.*, Vol. 19, 295–308, 1971.
3. Eisenhart, R. L. and P. J. Khan, "Theoretical and experimental analysis of a waveguide mounting structure," *IEEE Trans. Microwave Theory Tech.*, Vol. 19, 706–719, 1971.
4. Petlenko, V. A. and M. V. Nesterenko, "Current distribution and resonance of rod conductors in a rectangular waveguide," *Radiophysics Quantum Electronics*, Vol. 27, 236–241, 1984.
5. Lopuch, S. L. and T. K. Ishii, "Field distribution of two conducting posts in a waveguide," *IEEE Trans. Microwave Theory Tech.*, Vol. 32, 29–33, 1984.
6. Williamson, A. G., "Variable-length cylindrical post in a rectangular waveguide," *IEE Proceedings*, Vol. 133, Pt. H, 1–9, 1986.

7. Hashemi-Yeganeh, S. and C. R. Birtcher, "Numerical and experimental studies of current distributions on thin metallic posts inside rectangular waveguides," *IEEE Trans. Microwave Theory Tech.*, Vol. 42, 1063–1068, 1994.
8. Roelvink, J. and A. G. Williamson, "Reactance of hollow, solid, and hemispherical-cap cylindricalposts in rectangular waveguide," *IEEE Trans. Microwave Theory Tech.*, Vol. 53, 3156–3160, 2005.
9. Kirilenko, A., D. Kulik, L. Mospan, and L. Rud, "Two notched band two post waveguide," *Proc. of 12th Int. Math. Methods Electromagn. Theory Conf.*, 164–166, 2008.
10. Tomassoni, C. and R. Sorrentino, "A new class pseudoelliptic waveguide filters using dual-post resonators," *IEEE Trans. Microwave Theory Tech.*, Vol. 61, 2332–2339, 2013.
11. Cassedy, E. S. and J. Fainberg, "Back scattering cross sections of cylindrical wires of finite conductivity," *IEEE Trans. Antennas Propagat.*, Vol. 8, 1–7, 1960.
12. King, R. W. P. and T. T. Wu, "The imperfectly conducting cylindrical transmitting antenna," *IEEE Trans. Antennas and Propagat.*, Vol. 14, 524–534, 1966.
13. Lamensdorf, D., "An experimental investigation of dielectric-coated antennas," *IEEE Trans. Antennas Propagat.*, Vol. 15, 767–771, 1967.
14. Inagaki, N., O. Kukino, and T. Sekiguchi, "Integral equation analysis of cylindrical antennas characterized by arbitrary surface impedance," *IEICE Trans. Commun.*, Vol. 55-B, 683–690, 1972.
15. Bretones, A. R., R. G. Martín, and I. S. García, "Time-domain analysis of magnetic-coated wire antennas," *IEEE Trans. Antennas Propagat.*, Vol. 43, 591–596, 1995.
16. Nesterenko, M. V., "The electromagnetic wave radiation from a thin impedance dipole in a lossy homogeneous isotropic medium," *Telecommunications and Radio Engineering*, Vol. 61, 840–853, 2004.
17. Hanson, G. W., "Radiation efficiency of nano-radius dipole antennas in the microwave and far-infrared regimes," *IEEE Antennas Propagat. Mag.*, Vol. 50, No. 3, 66–77, 2008.
18. Nesterenko, M. V., V. A. Katrich, Yu. M. Penkin, V. M. Dakhov, and S. L. Berdnik, *Thin Impedance Vibrators. Theory and Applications*, Springer Science+Business Media, New York, 2011.
19. Lewin, L., *Theory of Waveguides. Techniques for the Solution of Waveguide Problems*, Newnes-Butterworths, London, 1975.
20. Gorobets, N. N., M. V. Nesterenko, V. A. Petlenko, and N. A. Khizhnyak, "Thin impedance vibrator in a rectangular waveguide," *Radio Eng.*, Vol. 39, 65–68, 1984.
21. Gorobets, N. N., M. V. Nesterenko, and V. A. Petlenko, "Resonance characteristics of thin impedance dipoles in a cutoff rectangular waveguide," *Telecommunications Radio Eng.*, Vol. 45, No. 4, 110–112, 1990.
22. Penkin, D. Yu, V. A. Katrich, Yu. M. Penkin, M. V. Nesterenko, V. M. Dakhov, and S. L. Berdnik, "Electrodynamic characteristics of a radial impedance vibrator on a perfect conduction sphere," *Progress In Electromagnetics Research B*, Vol. 62, 137–151, 2015.
23. Penkin, Yu. M., V. A. Katrich, M. V. Nesterenko, S. L. Berdnik, and V. M. Dakhov, *Electromagnetic Fields Excited in Volumes with Spherical Boundaries*, Springer Nature Swizerland AG, Cham, Swizerland, 2019.
24. Wu, T. T. and R. W. P. King, "The cylindrical antenna with nonreflecting resistive loading," *IEEE Trans. Antennas Propag.*, Vol. 13, 369–373, 1965.
25. Shen, L.-C., "An experimental study of the antenna with nonreflecting resistive loading," *IEEE Trans. Antennas Propagat.*, Vol. 15, 606–611, 1967.
26. Taylor, C. D., "Cylindrical transmitting antenna: Tapered resistivity and multiple impedance loadings," *IEEE Trans. Antennas Propagat.*, Vol. 16, 176–179, 1968.
27. Rao, B. L. J., J. E. Ferris, and W. E. Zimmerman, "Broadband characteristics of cylindrical antennas with exponentially tapered capacitive loading," *IEEE Trans. Antennas Propagat.*, Vol. 17, 145–151, 1969.

28. Yeliseyeva, N. P., S. L. Berdnik, V. A. Katrich, and M. V. Nesterenko, "Electrodynamic characteristics of horizontal impedance vibrator located over a finite-dimensional perfectly conducting screen," *Progress In Electromagnetics Research B*, Vol. 63, 275–288, 2015.
29. Garb, H. L., P. Sh. Friedberg, and I. M. Yakover, "Diffraction of an H_{10}-wave on a thin resistive film with a stepwise change of surface impedance in a rectangular waveguide," *Radioengineering Electronics*, Vol. 30, 41–48, 1985 (in Russian).
30. Miek, D., P. Boe, F. Kamrath, and M. Höft, "Techniques for the generation of multiple additional transmission zeros in H-plane waveguide filters," *International Journal of Microwave and Wireless Technologies*, 723–732, 2020.
31. Khizhnyak, N. A., *Integral Equations of Macroscopical Electrodynamics*, Naukova dumka, Kiev, 1986 (in Russian).